Modeling of quenching process in steel cylinders

Pedro Manuel Calas Lopes Pacheco, Luís Felipe Guimarães de Souza
CEFET/RJ - Department of Mechanical Engineering, Rio de Janeiro, RJ – Brazil
Marcelo Amorim Savi, Wendell Porto de Oliveira
Universidade Federal do Rio de Janeiro - COPPE - Department of Mechanical Engineering, Rio de Janeiro, RJ – Brazil
Eduardo Prieto Silva
Volkswagen do Brasil - Truck & Bus – DCT Chassis, Resende, RJ – Brazil

Abstract

This article deals with the modeling and simulation of quenching in steel cylinders using a multi-phase constitutive model with internal variables formulated within the framework of continuum mechanics and the thermodynamics of irreversible processes. Phenomenological aspects of quenching involve couplings among different physical processes and its description is unusually complex. Basically, three couplings are essential: thermal, phase transformation and mechanical phenomena. A numerical procedure is developed based on the operator split technique associated with an iterative numerical scheme in order to deal with non-linearities in the formulation. The proposed general formulation is applied to the quenching of steel cylinders. Three examples considering progressive induction hardening and through hardening are presented. Numerical results present a good agreement with those of experimental data obtained by the authors in previous works.

Keywords: quenching, phase transformation, thermomechanical coupling, modeling.

1 Introduction

Quenching is a heat treatment usually employed in industrial processes. It provides a mean to control some mechanical properties of steels as tensile strength, toughness and hardness. The process consists of raising the steel temperature above a certain critical value, holding it at that temperature for a fixed time and then rapidly cooling it in a suitable medium to room temperature. The phases and constituents formed from quenching results in different microstructures (ferrite, cementite, pearlite, upper bainite, lower bainite and martensite) which depend on cooling rate and on chemical composition of the steel. The volume variation associated with phase transformation combined with large temperature gradients and non-uniform cooling can promote high residual stresses in quenched steels. As these internal stresses can produce warping and even cracking of a steel body, the prediction of

Mechanics of Solids in Brazil 2007, Marcílio Alves & H.S. da Costa Mattos (Editors)
Brazilian Society of Mechanical Sciences and Engineering, ISBN 978-85-85769-30-7

such stresses is an important task [1–9]. Nevertheless, the proposed models are not generic and are usually applicable to simple geometries.

Phenomenological aspects of quenching involve couplings among different physical processes and its description is unusually complex. Basically, three couplings are essential: thermal, phase transformation and mechanical phenomena. The description of each one of these phenomena has been addressed by several authors by considering these aspects separately. Sen *et al.* [7] considers steel cylinders without phase transformations. There are also references that focus on the modeling of the phase transformation phenomenon [8, 10–12]. Several authors have proposed coupled models that are not generic and are usually applicable to simple geometries as cylinders [1–6, 13–15]. Moreover, there are some complex aspects that are usually neglected in the analysis of quenching process. As an example, one could mention the heat generated during phase transformation. This phenomenon is usually treated by means of the latent heat associated with phase transformation [3, 6, 13, 15, 16]. Meanwhile, other coupling terms in the energy equation related to other phenomena as plastic strain or hardening are not treated in literature and their analysis is an important topic to be investigated. Silva *et al.* [17] analyses the thermomechanical coupling during quenching considering austenite-martensite phase transformations. Silva *et al.* [18] employ the finite element method to study the phase transformation effect in residual stresses generated by quenching in notched steel cylinders.

This article deals with the modeling and simulation of quenching in steel cylinders using a multiphase constitutive model with internal variables formulated within the framework of continuum mechanics and the thermodynamics of irreversible processes. A numerical procedure is developed based on the operator split technique associated with an iterative numerical scheme in order to deal with non-linearities in the formulation. With this assumption, the coupled governing equations are solved to obtain the temperature, stress and phase fields from four uncoupled problems: thermal, phase transformation, thermoelastic and elastoplastic. Classical numerical methods are applied to the uncoupled problems. The proposed general formulation is applied to the quenching of steel cylinders. Three examples considering progressive induction hardening and through hardening are presented. Numerical results present a good agreement with those of experimental data obtained by the authors in previous works.

2 Phenomenological aspects of phase transformations

In quenching process, a steel piece is heated and maintained at constant temperature until austenite is obtained. Afterwards, a cooling process promotes the transformation of austenite phase into different phases and constituents which results in microstructures as: ferrite, cementite, pearlite, upper bainite, lower bainite and martensite. It can be observed that the microstructure of carbon alloy steel, depending on its chemical composition, can be composed by phases (austenite, ferrite, cementite and martensite) and constituents (pearlite, upper bainite and lower bainite). In order to describe all these microstructures in a macroscopically point of view, the volumetric fraction of each one of the phases and constituents of these microstructures is represented by β_i (austenite $i = A$, ferrite $i = 1$, cementite $i = 2$, pearlite $i = 3$, upper bainite $i = 4$, lower bainite $i = 5$ and martensite $i = M$). All of these microstructural constituents and phases may coexist, satisfying the following constraints: $\beta_A + \beta_1 +$

Mechanics of Solids in Brazil 2007, Marcílio Alves & H.S. da Costa Mattos (Editors)
Brazilian Society of Mechanical Sciences and Engineering, ISBN 978-85-85769-30-7

$\beta_2 + \beta_3 + \beta_4 + \beta_5 + \beta_M = 1$ and $0 \leq \beta_i \quad \leq 1$.

Phase transformation from austenite to martensite is usually considered as a non-diffusive transformation, which means that amount of volumetric phase is only a function of temperature [8, 11, 12]. This process may be described by the equation proposed by [19] and the evolution of martensitic phase can be written in a rate form as follows [20–22]:

$$\dot{\beta}_M\left(T,\dot{T}\right) = \varsigma_{A\to M}\,\beta_A^0\left[(1-\beta_M)\left(k\dot{T}\right)\right] \quad ; \quad \varsigma_{A\to M}\left(\dot{T},T\right) = \Gamma\left(-\dot{T}\right)\,\Gamma\left(M_s - T\right)\,\Gamma\left(T - M_f\right) \tag{1}$$

where β_A^0 is the amount of austenite at the beginning of transformation, k is a material property, T is the temperature and $\Gamma(x)$ is the Heaviside function. Under a stress-free state, M_s and M_f are the temperatures where martensitic transformation starts and finishes its formation.

Pearlite, cementite, ferrite and bainite formations are usually considered as diffusion-controlled transformation, which means that they are time dependent. The evolution of these phase transformations can be predicted through an approximate solution using data from Time-Temperature-Transformation diagrams (*TTT*) [8, 12] and considering that the cooling process may be represented by a curve divided in a sequence of isothermal steps where the phase evolution is calculated considering isothermal transformation kinetics expressed by a *JMAK* law [8, 12, 23, 24]. The rate form of volumetric phase i can be written as follows [20–22]:

$$\dot{\beta}_i = \varsigma_{A\to phase\ (i)}\left\{N_i(b_i)^{(1/N_i)}\left(\hat{\beta}_i^{\max}-\beta_i\right)\left[\ln\left(\frac{\hat{\beta}_i^{\max}}{\hat{\beta}_i^{\max}-\beta_i}\right)\right]^{\left(1-\frac{1}{N_i}\right)}\right\} \quad (i=1,...,5) \tag{2}$$

where N_i is the Avrami exponent and b_i is a parameter that characterizes the rate of nucleation and growth processes (Avrami, 1940; Reti *et al.*, 2001). $\hat{\beta}_i^{\max} = \beta_i^{\max}\left[\sum_{j=1;j\neq i}^{5}\beta_j - \beta_M\right]$ $(i = 1, ..., 5)$ where $\beta_i^{\max}$ represents the maximum volumetric fraction for a phase i and $\varsigma_{A\to phase\ (i)}\left(\dot{T},t\right) = \Gamma\left(-\dot{T}\right)\,\Gamma\left(t_i^f - t\right)\,\Gamma\left(t - t_i^s\right)$.

3 Constitutive model

Constitutive equations may be formulated within the framework of continuum mechanics and the thermodynamics of irreversible processes, by considering thermodynamic forces, defined from the Helmholtz free energy, ψ, and thermodynamic fluxes, defined from the pseudo-potential of dissipation, ϕ [25, 26].

The proposed phenomenological quenching model allows one to identify different aspects related to quenching process. With this aim, a Helmholtz free energy is proposed as a function of observable variables, total strain, ε_{ij}, and temperature, T. Moreover, the following internal variables are considered: plastic strain, ε_{ij}^p, volumetric fractions of seven different microstructures, represented by phases

in a macroscopic point of view, $\beta = (\beta_A,\ \beta_1,\ \beta_2,\ \beta_3,\ \beta_4,\ \beta_5,\ \beta_M)$. A variable related to kinematic hardening, α_{ij}, is also considered. Therefore, the following free energy is proposed, employing indicial notation where summation convention is evoked, except when indicated [20–22]:

$$\rho\psi(\varepsilon_{ij},\varepsilon^p_{ij},\alpha_{ij},\beta,T) = W(\varepsilon_{ij},\varepsilon^p_{ij},\alpha_{ij},\beta,T) = W_e(\varepsilon_{ij}-\varepsilon^p_{ij},\beta,T) + W_\alpha(\alpha_{ij}) + W_\beta(\beta) - W_T(T) \quad (3)$$

where ρ is the material density. The elastic strain can be written assuming an additive decomposition: $d\varepsilon^e_{ij} = d\varepsilon_{ij} - d\varepsilon^p_{ij} - \alpha_T dT\delta_{ij} - d\varepsilon^{tv}_{ij} - d\varepsilon^{tp}_{ij}$. In the right hand side of this expression, the first term is the total strain while the second is related to plastic strain. The third term is associated with thermal expansion. The parameter α_T is the coefficient of linear thermal expansion, T_0 is a reference temperature and δ_{ij} is the Kronecker delta. The fourth term is related to volumetric expansion associated with phase transformation from a parent phase $d\varepsilon^{tv}_{ij} = (\sum_{r=1}^{6}\gamma_r d\beta_r)\delta_{ij}$, where γ_r is a material phase property related to total expansion and $\beta_6 = \beta_M$. Finally, the last term is denoted as transformation plasticity strain $d\varepsilon^{tp}_{ij} = \sum_{r=1}^{6}\frac{3}{2}\kappa_r\, f'(\beta_r)d\beta_r\,\sigma^d_{ij}$, being the result of several physical mechanisms related to local plastic strain promoted by the phase transformation [1, 2]; κ_r is a material phase parameter, $f(\beta_r)$ expresses the transformation process dependence and σ^d_{ij} the deviatoric stress defined by $\sigma^d_{ij} = \sigma_{ij} - \delta_{ij}(\sigma_{kk}/3)$, with σ_{ij} being the stress tensor component. It should be emphasized that this strain may be related to stress states that are inside the yield surface.

In order to describe dissipation processes, it is necessary to introduce a potential of dissipation or its dual, which can be split into two parts $\phi^*(P_{ij},Q_{ij},R_{ij},X_{ij},B^\beta,g_i) = \phi^*_I(P_{ij},Q_{ij},R_{ij},X_{ij},B^\beta) + \phi^*_T(g_i)$:

The set of constitutive equations is composed by the thermodynamics forces (σ_{ij}, P_{ij}, X_{ij}, $B^{\beta i}$, s), associated with state variables ($\varepsilon_{ij}\varepsilon^p_{ij}, \alpha_{ij},\beta,T$), and the thermodynamic fluxes:

$$\sigma_{ij} = \frac{\partial W}{\partial\varepsilon_{ij}} = E_{ijkl}\varepsilon^e_{kl} \quad ; \quad Q_{ij} = -\frac{\partial W}{\partial\varepsilon^{tv}_{ij}} = \sigma_{ij} \quad ; \quad R_{ij} = -\frac{\partial W}{\partial\varepsilon^{tp}_{ij}} = \sigma_{ij} \quad ; \quad P_{ij} = -\frac{\partial W}{\partial\varepsilon^{p}_{ij}} = \sigma_{ij} \quad (4)$$

$$X_{ij} = \frac{\partial W}{\partial\alpha_{ij}} = H_{ijkl}\alpha_{kl} \quad ; \quad s = -\frac{1}{\rho}\frac{\partial W}{\partial T} \quad ; \quad B^{\beta_i} = -\frac{\partial W}{\partial\beta_i} = -Z_i \quad (i=1,...,5) \quad (5)$$

$$\dot\varepsilon^p_{ij} \in \partial_{P_{ij}} I^*_m(P_{ij},X_{ij}) = \lambda sign\,(\sigma_{ij} - H_{ijkl}\alpha_{kl}) \quad ; \quad \dot\alpha_{ij} \in -\partial_{X_{ij}} I^*_m(\sigma_{ij},X_{ij}) = \dot\varepsilon^p_{ij} \quad (6)$$

$$\dot\varepsilon^{tv}_{ij} = \frac{\partial\phi^*}{\partial Q_{ij}} = \sum_{r=1}^{6}\gamma_r\dot\beta_r\delta_{ij} \quad ; \quad \dot\varepsilon^{tp}_{ij} = \frac{\partial\phi^*}{\partial R_{ij}} = \sum_{r=1}^{6}\frac{3}{2}\kappa_r f'\,(\beta_r)\,\dot\beta_r\sigma^d_{ij} \quad (7)$$

$$\dot\beta_i = \frac{\partial\phi^*}{\partial B^{\beta_i}} = \varsigma_{A\to phase\ (i)}\left\{ N_i(b_i)^{(1/N_i)}\,(\beta_i^{\max}-\beta_i)\left[\ln\left(\frac{\beta_i^{\max}}{\beta_i^{\max}-\beta_i}\right)\right]^{\left(1-\frac{1}{N_i}\right)}\right\} \quad (i=1,2,3,4,5) \quad (8)$$

$$\dot\beta_6 = \frac{\partial\phi^*}{\partial B^{\beta_6}} = \varsigma_{A\to M}\left[(1-\beta_6)\,k\dot T\right] \quad ; \quad q_i = -\frac{\partial\phi^*}{\partial g_i} = -\Lambda T\ g_i = -\Lambda\frac{\partial T}{\partial x_i} \quad (9)$$

where $Z_i \in \partial_\beta I_\beta(\beta)$ is the sub-differential of the indicator function I_β, $\mathrm{sign}(x) = x\ /\ |x|$, λ is the plastic multiplier from the classical theory of plasticity [27] and q_i is the heat flux vector. By assuming

that the specific heat is $c = -(T/\rho)\ \partial^2 W/\partial T^2$ and the set of constitutive equations (4-9), the energy equation can be written as [28]:

$$\frac{\partial}{\partial x_i}\left(\Lambda\frac{\partial T}{\partial x_i}\right) - \rho c\dot{T} = -a_I - a_T \quad ; \quad \begin{cases} a_I = \displaystyle\sum_{r=1}^{6} B^{\beta_r}\dot{\beta}_r - X_{ij}\dot{\varepsilon}^p_{ij} + \sigma_{ij}\left(\dot{\varepsilon}^p_{ij} + \dot{\varepsilon}^{tv}_{ij} + \dot{\varepsilon}^{tv}_{ij}\right) \\ a_T = T\left[\dfrac{\partial \sigma_{ij}}{\partial T}\left(\dot{\varepsilon}_{ij} - \dot{\varepsilon}^p_{ij} - \dot{\varepsilon}^{tp}_{ij} - \dot{\varepsilon}^{tv}_{ij}\right) - \displaystyle\sum_{r=1}^{6}\frac{\partial B^{\beta_r}}{\partial T}\dot{\beta}_r + \frac{\partial X_{ij}}{\partial T}\dot{\varepsilon}^p_{ij}\right] \end{cases} \tag{10}$$

Terms a_I and a_T are, respectively, internal and thermal coupling. The first one is always positive and has a role in the energy equation similar to a heat source in the classical heat equation for rigid bodies. The thermomechanical coupling effect related to phase transformation may be represented as a latent heat released during the phase transformation [5, 6, 15]: $a_I + a_T = \dot{Q} = \sum_{i=1}^{6} \Delta H_i\ \dot{\beta}_i$ where ΔH_i is the enthalpy variation in a transformation process involving a previous phase (austenite) and a product phase β_i (i = 1, ..,6). Therefore, this source term is used instead of all thermomechanical couplings effects, which represents a first approach of the general formulation [17].

4 Cylindrical bodies

This contribution considers cylindrical bodies as an application of the proposed general formulation. Two models are considered. The first one is a one-dimensional model based on the finite difference method that can be applied to homogeneous long cylinders. With this assumption, heat transfer analysis may be reduced to a one-dimensional problem. Moreover, plane stress or plane strain state can be assumed. Under these assumptions, only radial, r, circumferential, θ, and longitudinal, z, components need to be considered and a one-dimensional model is formulated. For this case, tensor quantities presented in the previous section may be replaced by scalar or vector quantities. As examples, one could mention: E_{ijkl} replaced by E; H_{ijkl} replaced by$H$; σ_{ij} replaced by σ_i (σ_r, σ_θ , σ_z). The second one is an axisymmetric finite element model and can be used to study more complex geometries like notched cylinders. A detailed description of these simplifications could be found in [17, 18, 21, 25, 26, 29].

The numerical procedure here proposed is based on the operator split technique [28] associated with an iterative numerical scheme in order to deal with non-linearities in the formulation. With this assumption, coupled governing equations are solved from four uncoupled problems: thermal, phase transformation, thermo-elastic and elastoplastic.

Thermal Problem - Comprises a conduction problem with convection and radiation. Material properties depend on temperature, and therefore, the problem is governed by non-linear parabolic equations. An implicit finite difference predictor-corrector procedure or the finite element method is used for numerical solution [28, 30, 31].

Phase Transformation Problem – The volumetric fractions of the phases are determined in this problem. Evolution equations are integrated from a simple implicit Euler method [30].

Thermo-elastic Problem - Stress and displacement fields are evaluated from temperature distribution. Numerical solution is obtained employing a shooting method procedure or the finite element method [30].

Elastoplastic Problem - Stress and strain fields are determined considering the plastic strain evolution in the process. Numerical solution is based on the classical return mapping algorithm [32].

5 Numerical simulations

As an application of the general proposed model, three numerical investigations associated with the quenching of long steel cylindrical bars of SAE 4140H steel with radius R are carried out. Numerical simulations include progressive induction hardening (PIH) and through hardening (TH). PIH is a heat treatment process carried out by moving a workpiece at a constant speed through a coil and a cooling ring. Applying an alternating current to the coil, a magnetic field is generated inducing eddy currents that heats the workpiece and promotes the formation of a thin surface layer of austenite. Afterwards, a cooling fluid is sprayed on the surface by the cooling ring promoting the quenching of the layer, which is transformed into martensite, pearlite, bainite and proeutectoid ferrite depending on, among other things, the cooling rate. A hard surface layer with high compressive residual stresses, combined with a tough core with tensile residual stresses, is often obtained. TH consists of heating the steel, usually in a furnace, to a suitable austenitizing temperature, holding at that temperature for a sufficient time to effect the desired change in crystalline structure, and immersing and cooling in a suitable liquid medium.

Material parameters of the cylinder are the following [1–3, 6, 14]: $\gamma_1 = 3.333\text{x}10^{-3}$, $\gamma_2 = 0$, $\gamma_3 = \gamma_4 = \gamma_5 = 5.000\text{x}10^{-3}$, $\gamma_6 = 1.110$ x 10^{-2}, $\kappa_i = (5/(2\sigma_y^A))\gamma_i$ (where σ_y^A is the austenite yielding stress and i = 1,2,3,4,5,6), $\rho = 7.800$ x 10^3 Kg/m^3, $M_s = 370\ ^\circ$C, $M_f = 260\ ^\circ$C. Other parameters depend on temperature and needs to be interpolated from experimental data. Therefore, parameters E, H, σ_Y, α_T, c, Λ and the convection coefficient, h, are evaluated by polynomial expressions [14, 25, 26, 33]. Temperature dependent parameters for diffusive phase transformations presented in Section 2 are obtained from *TTT* diagrams [34]. Moreover, latent heat released associated with the enthalpy variation in a transformation process involving a parent phase (austenite) and a product phase β_i (i = 1, ...,6) are given by: $\Delta H_1 = 1.55 \times 10^9$ - $(2.31 \times 10^4)T + 15.97T^2 - (4.29 \times 10^{-3})T^3$ - $(5.00 \times 10^9)/T$ J/m^3, $\Delta H_3 = 1.56 \times 10^9$ - $(1.5 \times 10^6)T$ J/m^3, $\Delta H_6 = 640 \times 10^6$ J/m^3 [6, 15].

At first, results from PIH simulations using the one-dimensional finite difference model with non-diffusive phase transformations (austenite-martensite) [25, 26]. PIH simulations regards a cylinder with a radius R = 22.5 mm, where a 5 mm thickness layer is heated to 850 $^\circ$C for 10 s and then, immersing in a liquid medium at 20 $^\circ$C until time instant 120 s is reached. Experimental results for PIH in cylindrical bodies, discussed in [35] and [25, 26] are used as reference for the comparison with numerical results here obtained. Experimental results, obtained for similar conditions, furnish circumferential (σ_θ) and longitudinal (σ_z) residual stress values at the surface of -830 MPa and -500 MPa, respectively. These values, measured through X-ray diffraction technique, present an uncertainty of 30 MPa. Moreover, hardness measurements and metallographic analysis are performed to identify the martensitic hardened layer.

Temperature time history for different positions of the cross-section is presented in Figure 1a. Notice that for layers deeper than 5 mm, temperature does not reach austenitizing limit. The stress distribution over the radius for the final time instant is presented in Figure 1b. Notice the stress values on the external surface, $\sigma_\theta = -866$ MPa and $\sigma_z =$ -255 MPa. The circumferential stress, σ_θ, is close to experimental results. The longitudinal stress, σ_z, on the other hand, presents a discrepancy that could be explained by the assumption of plane strain state adopted to simulate the restriction associated with adjacent regions of the heated region, which is at lower temperatures.

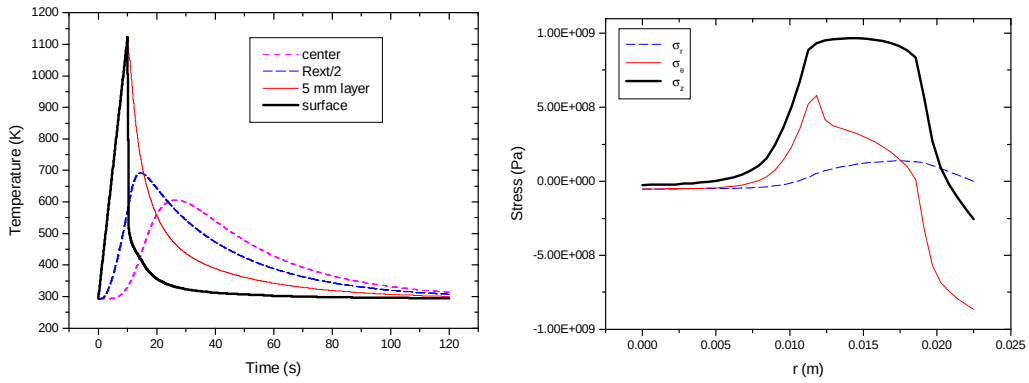

(a) (b)

Figure 1: PIH quenched cylinder ($R = 22.5$ mm): (a) Temperature time history for different positions and (b) stress distribution for final time instant.

Figure 2a shows a cross-section of a quenched bar submitted to a Nital 2% etch, while Figure 2b presents its hardness measures. In order to compare numerical and experimental results, a relation between volume fraction of phases and hardness is established. Therefore, it is assumed that martensitic phase (β_6) has 60 HR_C while a value of 30 HR_C is adopted for the regions where martensitic phase is absent, that is, this value is considered as a mean value of hardness among the other phases. Figure 2c presents the martensite volumetric fraction distribution for final time instant. The process quenches only points from external surface to 3 mm deep. Outside this region, retained austenite is observed. Once again, numerical results predicted by the model are close to experimental data.

The proposed model can be used as a powerful tool to predict the thermomechanical behavior of quenched mechanical components and choose important parameters as the cooling medium and the induced layer thickness. Figure 3 shows the longitudinal stress distribution and the volume fraction of martensite distribution for five thickness values of induced layers (PI) and for a through hardening (TH). The simulation of through hardening concerns a body with homogeneous temperature 1120K (850 $^\circ$ C) which are immersed in a liquid medium with 293K (20 $^\circ$ C) until a time instant 150 s is reached. The cooling medium is the same that is used on surface hardening. Since longitudinal direction

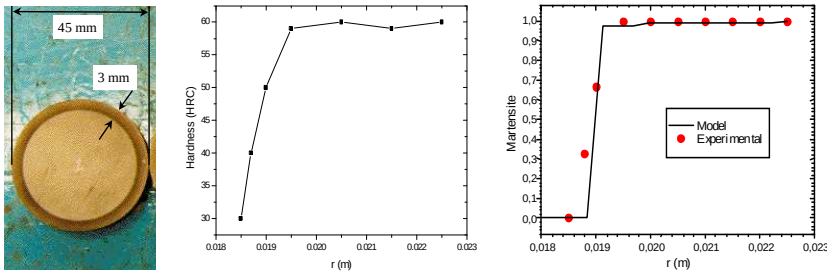

(a) (b) (c)

Figure 2: PIH quenched cylinder ($R = 22.5$ mm): (a) Cross-section view (Nital 2% etch), (b) hardness measures and (c) and martensite volumetric fraction distribution for final time instant.

is free, a plane stress state is adopted.

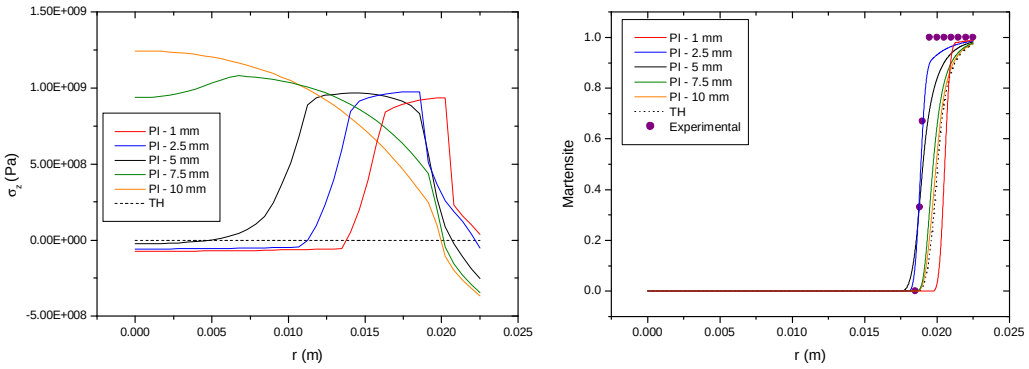

(a) (b)

Figure 3: Induced layer thickness. Longitudinal stress distribution (a) and distribution of volume fraction of martensite (b) for final time instant.

Results show that the thickness of the induced layer is an important parameter on the residual stress distribution. Higher thickness values promote higher stress at the center and lower stress at the surface. For the thinner induced layer (1 mm), a positive value of σ_z (about 40 MPa) is observed at the surface. This is a condition that must be avoided, as a traction stress field on the surface can promote the growth of surface defects.

In the forthcoming, experimental analyses developed by the authors to study the thermomechanical coupling influence on the evolution of the temperature and the phases volumetric fractions are pre-

sented [20–22]. The experimental procedure consists of heating cylindrical specimens of SAE 4140H with 2" of diameter in a furnace to a suitable austenitizing temperature (830 ° C), holding at that temperature for a sufficient time for the alloy to completely transform to austenite in all parts of the workpiece (1 hour), and finally cooling in air. Four cylindrical specimens are used: one with two holes and three with one hole at the center. Thermocouples are introduced at each hole and the temperature time history is acquired and registered by a data acquisition system. Figure 4 shows the furnace, the data acquisition system and the cylindrical specimen.

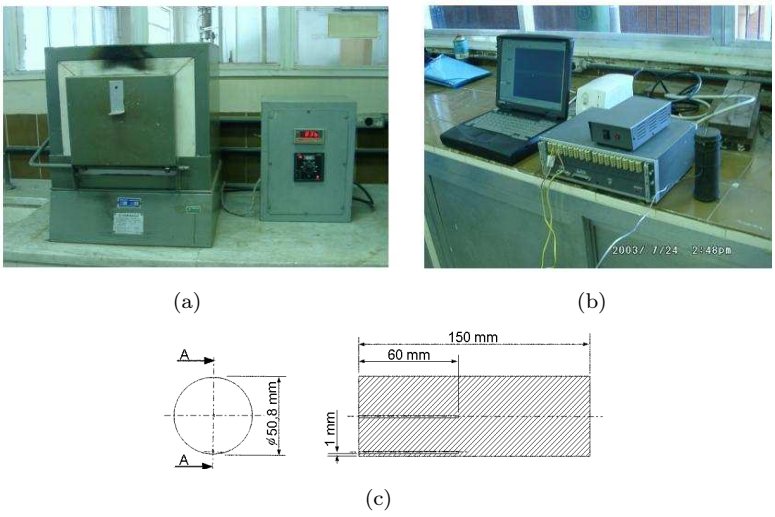

Figure 4: (a) Furnace, (b) data acquisition system and (c) cylindrical specimen.

At this point, two models are considered: *uncoupled* and *coupled*. The uncoupled model neglects the thermomechanical couplings, corresponding to the rigid body energy equation. The coupled model considers the latent heat associated with phase transformation as a source in the energy equation. Both models consider the presence of non-diffusive and diffusive phases.

Figure 5 presents the temperature time history curves for both models. At a temperature about 650 ° C a temperature increase can be observed in Fig. 5b for the *coupled* model which is also observed in experimental data. This phenomenon is related to the thermomechanical coupling associated with the latent heat of the austenite → ferrite+cementite (pearlite) phase transformation [6, 17] and is not captured by the *uncoupled* model.

Figure 6 presents the phase distribution along the cylinder radius for both models. Experimental data obtained from metallographic analysis using the point count technique shows an almost homogeneous phase distribution along the radius: 26% ferrite and 74% pearlite, that is in close agreement with the *coupled* model prediction. The *uncoupled* model, on the other hand, does not fit the experi-

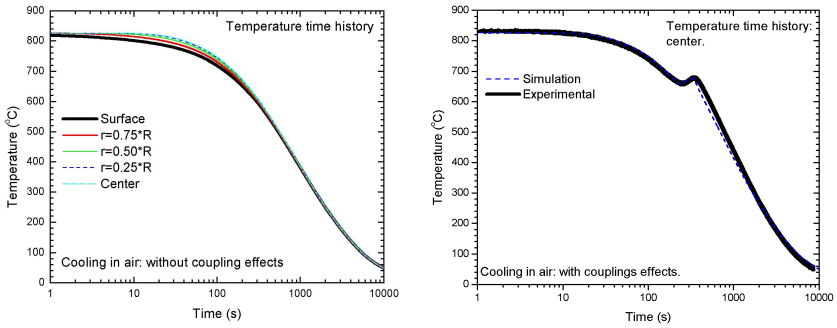

(a) (b)

Figure 5: Temperature evolution for (a) *uncoupled* and (b) *coupled* models.

mental data and upper bainite is predicted together with ferrite and pearlite. The formation of bainite (observed only by the *uncoupled* model prediction) is related to the faster cooling rate. Notice that the temperature time history observed in experimental data and also in numerical results predicted by the *coupled* model presents a temperature rise near 650 ° C which delays the cooling and avoids the bainitic formation.

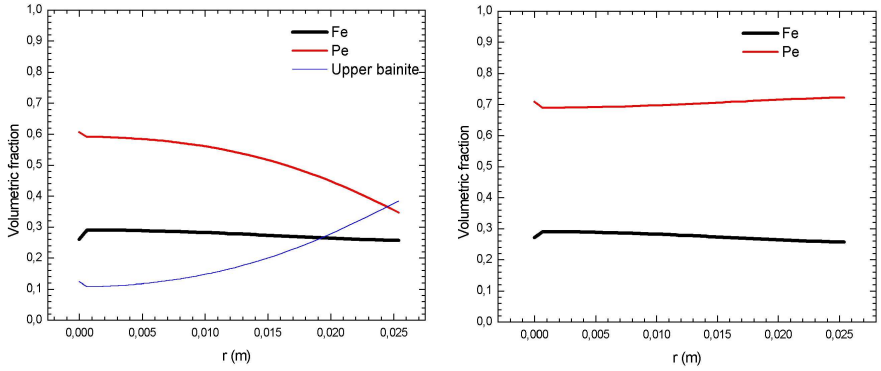

(a) (b)

Figure 6: Volumetric phase distribution for (a) *uncoupled* and (b) *coupled* models.

Finally, numerical simulations that explore the effect of austenite-martensite phase transformation in the determination of residual stresses in notched steel cylinders are presented [18]. In order to analyze the effect of phase transformation during quenching process, numerical investigations are carried

out simulating a PIH. Finite element analysis is performed exploiting a single strip axisymmetrical geometry for simulations. This assumption is employed since the passage of the moving workpiece through the heating and cooling rings promotes a localized phenomenon in this single strip while adjacent material, above and below this strip, is at lower temperatures.

With this aim, PIH of a steel cylinder, 45 mm diameter and 180 mm length, subjected to an induced layer thickness $e_{PI} = 3.5$ mm is considered. The specimen induced layer is heated to 1120K (850 $^\circ$ C) for 5s and then, the surface is sprayed by a liquid medium at 294K (21 $^\circ$ C) for 10 s. After that, the specimen is subjected to air-cooling until a time instant of 60s is reached. The cylinder has a notch with radius of 1 mm and a thickness of induced layer of 5 mm.

Residual stresses generated by quenching process is now focused on, comparing results predicted by two different models: *complete* (thermo-elastoplastic model with austenite-martensite phase transformation) and *without phase transformation* (thermo-elastoplastic model without phase transformation). Figure 8 shows *von Mises* residual stress distribution generated by quenching process. With this assumption, notice that the model neglecting phase transformation underestimate results when compared to the complete model. This difference is about 7.5% for maximum von Mises stresses. Figure 7 presents results predicted by both models, pointing out the difference between them. Notice that the complete model has a larger critical region.

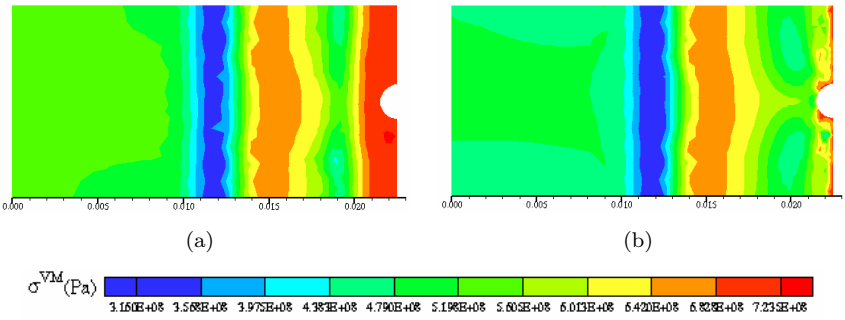

Figure 7: *von Mises* residual stresses. (a) *Complete* model; (b) Model *without phase transformation*.

At this point, it is analyzed data through the radius of the cylinder. Figure 8 presents a comparison between the results predicted by both models, showing that the notch introduces different perturbation in both models. Notice that far from the notch, where phase transformation does not occur, results predicted by both models are similar. Meanwhile, at the region between node 18 and the cylinder surface, the inclusion of phase transformation causes great discrepancies in the response of both models. Notice that the complete model predicts compressive values in the entire notch surface, except at the edges where small tensile values are observed. On the other hand, the model without phase transformation predicts tensile stresses in some regions of the notch surface. This can be an important data for assessing the structural integrity of a mechanical component subjected to fatigue loadings.

Since fatigue cracks usually initiate at the surface and propagate in the presence of tensile stress fields, tensile residual stresses at the surface can be especially critical.

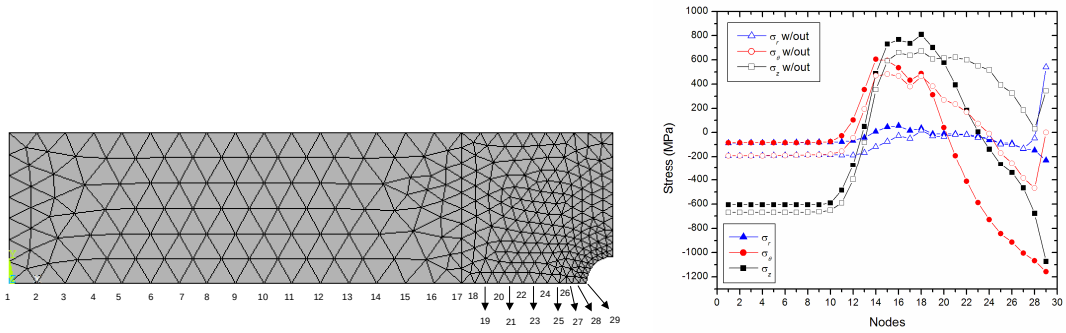

Figure 8: Residual stresses through the radius of the cylinder for both models.

6 Conclusions

The present contribution regards on modeling and simulation of quenching process, presenting an anisothermal multi-phase constitutive model formulated within the framework of continuum mechanics and thermodynamics of irreversible processes. This approach allows a direct extension to more complex situations, as the analysis of three-dimensional media. A numerical procedure is developed based on the operator split technique associated with an iterative numerical scheme in order to deal with non-linearities in the formulation. The proposed numerical procedure allows the use of traditional numerical methods, like the finite element method. Progressive induction hardening and through hardening of cylindrical bodies are considered as applications of the proposed general formulation. Numerical results show that the proposed model is capable of capturing the general behavior of experimental data. Therefore, it can be used as a powerful tool to predict the thermomechanical behavior of quenched mechanical components and choose important parameters as the cooling medium and the induced layer thickness.

Acknowledgements

The authors would like to acknowledge the support of the Brazilian Research Agencies CNPq and CAPES.

References

[1] Sjöström, S., Interactions and constitutive models for calculating quench stresses in steel. *Material Science and Technology*, **1**, pp. 823–829, 1985.

[2] Denis, S., Gautier, E., Simon, A. & Beck, G., Stress-phase-transformation interactions - basic principles - modelling and calculation of internal stresses. *Material Science and Technology*, **1**, pp. 805–814, 1985.

[3] Denis, S., Archambault, S., Aubry, C., Mey, A., Louin, J. & Simon, A., Modelling of phase transformation kinetics in steels and coupling with heat treatment residual stress predictions. *Journal de Physique IV*, **9**, pp. 323–332, 1999.

[4] Denis, S., Considering stress-phase transformation interaction in the calculation of heat treatment residual stresses. *Journal de Physique IV*, **6**, pp. 159–174, 1996.

[5] Fernandes, M., Denis, S. & Simon, A., Mathematical model coupling phase transformation and temperature evolution during quenching of steels. *Materials Science and Technology*, **1**, pp. 838–844, 1985.

[6] Woodard, P., Chandrasekar, S. & Yang, H., Analysis of temperature and microstructure in the quenching of steel cylinders. *Metallurgical and Materials Trans*, 1999.

[7] Sen, S., Aksakal, B. & Ozel, A., Transient and residual thermal stresses in quenched cylindrical bodies. *International Journal of Mechanical Sciences*, **42(10)**, pp. 2013–2029, 2000.

[8] Çetinel, H., Toparlı, M. & Özsoyller, &., A finite element based prediction of the microstructural evolution of steels subjected to the tempcore process. *Mechanics of Materials*, **32**, pp. 339–347, 2000.

[9] Gür, C. & Tekkaya, A., Numerical investigation of non-homogeneous plastic deformation in quenching process. *Materials Science and Engineerin*, **A319-321**, pp. 164–169, 2001.

[10] Hömberg, D., A numerical simulation of the jominy end-quench test. *Acta Mater*, **44(11)**, pp. 4375–4385, 1996.

[11] Chen, J., Tao, Y. & Wang, H., A study on heat conduction with variable phase transformation composition during quench hardening. *Journal of Materials Processing Technology*, **63**, pp. 554–558, 1997.

[12] Reti, T., Fried, Z. & Felde, I., Computer simulation of steel quenching process using a multi-phase transformation model. *Computational Materials Science*, **22**, pp. 261–278, 2001.

[13] Inoue, T. & Wang, Z., Coupling between stress, temperature, and metallic structures during processes involving phase transformations. *Material Science and Technology*, **1**, pp. 845–850, 1985.

[14] Melander, M., *A Computational and Experimental Investigation of Induction and Laser Hardening*. Ph.D. thesis, Department of Mechanical Eng. - Linkoping University, 1985.

[15] Denis, S., Sjöström, S. & Simon, A., Coupled temperature, stress, phase transformation calculation model numerical illustration of the internal stresses evolution during cooling of a eutectoid carbon steel cylinde. *A Metallurgical Transactions*, **18A**, pp. 1203–1212, 1987.

[16] Sjöström, S., (ed.), *Physical - Mathematical and Numerical Modelling for Calculation of Residual Stresses: Fundamentals and Applications*, Fourth International Conference on Residual Stresses: Baltimore - USA, 1994.

[17] Silva, E., Pacheco, P. & M.A.Savi, On the thermo-mechanical coupling in austenite-martensite phase transformation related to the quenching process. *International Journal of Solids and Structures*, **41(3-4)**, pp. 1139–1155, 2004.

[18] Silva, E., Pacheco, P. & M.A.Savi, Finite element analysis of the phase transformation effect in residual stresses generated by quenching in notched steel cylinders. *Journal of Strain Analysis for Engineering Design*, **40(2)**, pp. 151–160, 2005.

[19] Koistinen, D. & Marburger, R., A general equation prescribing the extent of the austenite-martensite transformation in pure iron-carbon alloys and plain carbon steels. *Acta Metallurgica*, **7**, pp. 59–60, 1959.

[20] Oliveira, W., Souza, L., Pacheco, P. & Savi, M., Quenching process modeling in steel cylinders using a multi-phase constitutive model. *COBEM 2003 - 17^{th} - International Congress of Mechanical Engineering*, 2003.

[21] Oliveira, W., *Modeling Quenching Process in Steel Cylinder Using Multi-Phase Constitutive Model*. Master's thesis, CEFET/RJ, 2004. In Portuguese.

[22] Oliveira, W., Savi, M., Pacheco, P. & de Souza, L., Finite element analysis of the thermomechanical coupling in quenching of steel cylinders using a constitutive model with diffusional phase transformations. *ECCM-2006 - III European Conference on Computational Mechanics*, Lisboa - Portugal, 2006.

[23] Avrami, M., Kinetics of phase change. ii: Transformation-time relations for random distribution of nuclei. *Journal of Chem Phys*, **8**, p. 212, 1940.

[24] Cahn, J., Transformation kinetics during continuous cooling. *Acta Metallurgica*, **4**, pp. 572–575, 1956.

[25] Pacheco, P., Savi, M. & ao, A.C., Analysis of residual stresses generated by progressive induction hardening of steel cylinders. *Journal of Strain Analysis for Engineering Design*, **36(5)**, pp. 507–516, 2001a.

[26] Pacheco, P., Savi, M. & ao, A.C., (eds.), *Quenching Generated Residual Stresses in Steel Cylinders*, XV Brazilian Congress of Mechanical Engineering – ABCM: Águas de Lindóia - Brazil, 2001b. (in Portuguese).

[27] Lemaitre, J. & Chaboche, J., *Mechanics of Solid Materials*. Cambridge Press Univ., 1990.

[28] Pacheco, P., *Analysis of Thermomechanical Coupling in Elasto-viscous-plastic Materials*. Ph.D. thesis, epartment of Mechanical Engineering - PUC-Rio, 1994.

[29] Silva, E., *Modeling and Simulation of Steel Quenching Process Using Finite Element Method*. Master's thesis, Department of Mechanical and Materials Engineering - Instituto Militar de Engenharia, 2002. In Portuguese.

[30] Ames, W., Numerical methods for partial differential equations. *Academic Press*, 1992.

[31] Lewis, R., Morgan, K., Thomas, H. & Seethramu, K., *The Finite Element Method in Heat Transfer Analysis*. John Wiley & Sons: USA, 1996.

[32] Simo, J. & Hughes, T., *Computational Inelasticity*. Springer, 1998.

[33] Hildenwall, B., *Prediction of the Residual Stresses Created During Quenching*. Ph.D. thesis, Linkoping Univ., 1979.

[34] ASM, Atlas of isothermal transformation and cooling transformation diagrams. *American Society Metals*, 1977.

[35] ao, A.C., *A Model to Predict Residual Stresses in the Progressive Induced Quenching of Steel Cylinders*. Ph.D. thesis, Department of Metallurgical and Materials Engineering - USP, 1998. In Portuguese.